Studies of Double-Layer Effects at Single-Crystal Gold Electrodes. 1. The Reduction Kinetics of Hexaamminecobalt(III) Ion in Aqueous Solutions

Magdaléna Hromadová and W. Ronald Fawcett*

Department of Chemistry, UC Davis, California 95616

Received: November 22, 1999; In Final Form: February 11, 2000

The effect of the double-layer on the reduction of $[Co(NH_3)_6]^{3+}$ cation has been studied at four different single-crystal gold substrates, namely, Au(111), Au(100), Au(110), and Au(210), and at various concentrations of perchloric acid. The values of the experimental transfer coefficient (α_{ex}) are much larger than 1.0 at all gold surfaces and decrease with increasing concentration of the supporting electrolyte. The value of α_{ex} also depends on the crystallographic orientation of the gold substrate and increases in the following order: Au(111) < Au(100) < Au(110) < Au(210), consistent with a decreasing reduction rate from Au(111) to Au(210) at constant electrode potential. The experimental transfer coefficients are rationalized on the basis of the classical theory of the double-layer with consideration of reactants and products in estimation of the diffuse-layer potential. The charge on the reactant transported through the double-layer is 2+. Corrected Tafel plots yield an apparent transfer coefficient α_a equal to 1.1 ± 0.1 for all analyzed substrates. Corrected rate constants for double-layer effects indicate that the reduction of $[Co(NH_3)_6]^{3+}$ ion depends on the crystallographic orientation of the gold substrate only through the differences in the potential of zero charge. This behavior confirms that the role of the metal is that expected for an adiabatic outer-sphere electron-transfer process.

Introduction

In recent years there has been considerable interest in fundamental studies of electron-transfer kinetics at well-defined solid metal electrodes. However, if one excludes studies of the reaction kinetics at chemically modified single-crystal electrodes, only a few experimental papers were published exploring the role of crystallographic orientation on electron-transfer kinetics in aqueous solutions.[1−11] This is partly due to the presence of reconstruction phenomena,[9] which constitute limitations at the experimental level, and also due to the lack of simple model systems with uncomplicated electrochemical and solution equilibria.

It is generally believed that, at least for simple outer-sphere adiabatic electron-transfer processes where the reactant does not penetrate the compact layer of water in the inner layer at the metal/electrolyte interface, the chemical nature of the electrode has no direct influence on the electron-transfer barrier. The only observable effect comes from the variations in the electrostatic work terms, that is, from double-layer effects. This statement directly suggests that different crystallographic orientations of chemically identical electrodes, such as used in the present work, should influence electron-transfer rates of adiabatic processes only through the differences in the electrostatic work terms, demonstrated by different potentials of zero charge (E_z).

Hamelin and Weaver[3] studied the one-electron reduction of $[Co(NH_3)_6]^{3+}$, $[Co(NH_3)_5F]^{2+}$, and $[Co(NH_3)_5OSO_3]^{+}$ in acidified 0.1 M $NaClO_4$ electrolyte at Au(111), Au(100), and Au(110) electrodes. These reactants are anticipated to reduce via outer-sphere pathways, but with very different double-layer effects due to the differences in ionic charge. The experimental (double-layer uncorrected) rate constants for $[Co(NH_3)_6]^{3+}$ and $[Co(NH_3)_5F]^{2+}$ ions were found to decrease in the order Au(111) > Au(100) > Au(110) at a constant potential of +0.1V against the SCE, whereas an opposite trend was found for $[Co(NH_3)_5OSO_3]^{+}$ at +0.3 V against the SCE. The double-layer corrected reaction rates at Au(111) were much higher than at mercury and the authors concluded that the reaction site at gold is closer to the metal than in the case of mercury.

Later, Hamelin and Weaver[4] studied the dependence of proton reduction kinetics on the crystallographic orientation of gold electrodes. The experimental rate constants increased in the sequence Au(111) < Au(100) < Au(332) < Au(110) < Au(311) < Au(210) at constant electrode potential. This trend was still present after correction for the double-layer contribution. Brug et al.[5] found the same trend in the experimental rate constants, but after correction for the double-layer contribution, the kinetics was only weakly dependent on the crystallographic orientation. Recently, the subject of the effect of crystallographic orientation of gold on the proton reduction was revisited by Perez et al.[6] These authors observed a completely opposite trend in the experimental rate constants. The hydrogen evolution occurred at the most positive potentials on Au(111) and the reduction rate increased in the order Au(110) < Au(100) < Au(111) at constant electrode potential. The kinetic data in all these cases were collected in solutions of high ionic strength between 0.1 and 1 M.

Fedorovich et al.[7] discussed the reduction of peroxodisulfate anion at Ag(111), Ag(100), and Bi(111) single-crystals. Corrected Tafel plots overlaped for all three single-crystals, demonstrating that change in the metal substrate only affected the potential drop across the diffuse layer. Samec et al.[8] found that the reduction of peroxodisulfate on gold electrodes can proceed via two pathways, but in the case of the direct pathway (no $S_2O_8^{2-}$ adsorption) they also did not observe any differences between the electron-transfer kinetics on the Au(111) and Au(110) electrodes after proper correction for the double-layer effects.

Fawcett et al.[9] recently found marked differences in the reduction kinetics of $[Co(NH_3)_6]^{3+}$ and $[Fe(H_2O)_6]^{3+}$ ions at

10.1021/jp994136z CCC: $19.00
Published on Web 04/14/2000

reconstructed and unreconstructed Au(100) electrodes. The observed effects were attributed to changes in the potential of zero charge during cycling of the electrode due to reconstruction phenomena. A more qualitative study of the double-layer effects on the reduction kinetics of $[Fe(H_2O)_6]^{3+}$ ions at Au(111), Au(100), and Au(110) was also published.[10] Samec[11] recently reported no significant changes in the kinetics of $[Fe(H_2O)_6]^{3+}$ reduction at Au(110) at different concentrations of supporting electrolyte. This behavior was attributed to the reaction site being located further from the electrode in a part of the diffuse layer where the double-layer effects are no longer significant.

It is evident from the literature that studies of the double-layer effects on the electron-transfer kinetics at single-crystal electrodes are important in assessing the role of the metal on electron-transfer. Many experimental studies conducted to date have minimized the effect of the double-layer by using high concentrations of the supporting electrolyte.

In the present paper, a study of the effect of the electric double-layer on the reduction of $[Co(NH_3)_6]^{3+}$ ion at different crystallographic orientations of superpurity gold is presented. The $[Co(NH_3)_6]^{3+}$ ion was chosen for its simple reduction behavior and uncomplicated one-electron *adiabatic outer-sphere* electron-transfer.[12,33,34] The single-crystal faces of gold were selected to achieve a large difference in the values of E_z. The previous work of Hamelin and Weaver[3] has been extended with quantitative estimation of the double-layer effects.

Experimental Section

A conventional three-electrode jacketed glass cell was used for all experiments. The working electrodes were single-crystal gold cylinders purchased from Metal Crystals and Oxides Ltd., Cambridge, UK. The electrode surface preparation consisted of polishing the rods with different sizes of alumina powder on a polishing wheel, flame annealing, and electropolishing in perchloric acid solution. The single-crystal made contact with the solution in the cell employing a hanging meniscus technique. The cleanliness of the solution and the quality of the electrode surface were verified by cyclic voltammetry. A calomel reference electrode filled with 0.05 M KCl solution ($CE_{0.05}$) and a gold counter electrode completed the three-electrode setup. The reference electrode was connected to the cell through a long (15 cm) Luggin capillary filled with the same $HClO_4$ solution as in the main cell compartment. This choice minimized possible contamination of the solution by chloride anions. The experiments were conducted at a constant temperature of 25 °C under an argon atmosphere.

All solutions were prepared with Nanopure water of maximum resistivity 18 MΩ/cm (Barnstead). Glassware was cleaned in boiling 50% nitric acid and washed with Nanopure water before each set of experiments. Perchloric acid (Acros Organics), sodium perchlorate (Fisher Scientific), $[Co(NH_3)_6]Cl_3$, and $[Ru(NH_3)_6]Cl_3$ (both Aldrich) were of the best quality available from the manufacturers. The reactants $[Co(NH_3)_6](ClO_4)_3$ and $[Ru(NH_3)_6](ClO_4)_3$ were prepared from the corresponding chlorides by precipitation with saturated sodium perchlorate and recrystallization from water.

Cyclic voltammograms (CVs) were obtained by using a Princeton Applied Research/PAR 173 potentiostat with a PAR 175 universal programmer employing positive feedback *iR* compensation. Data were collected in digitized form by using a PowerLab/4s four-channel analyzer (AD Instruments) connected to a personal computer or, more conventionally, with a Kipp & Zonen BD 91 X−Y recorder.

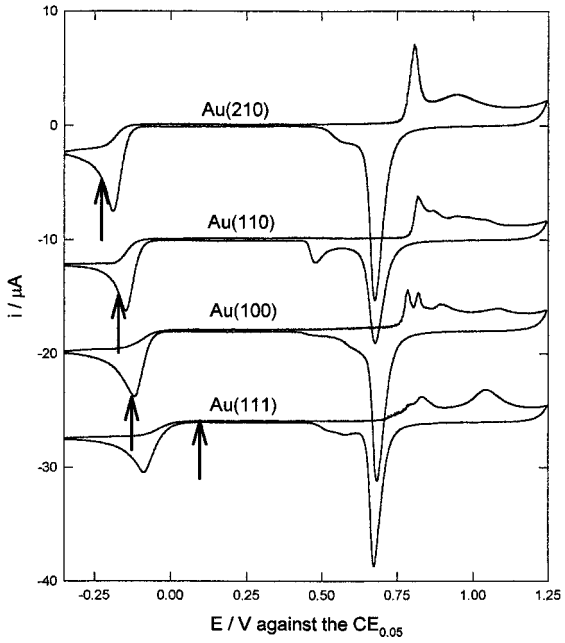

Figure 1. Cyclic voltammograms for the reduction of 5×10^{-4} M $[Co(NH_3)_6]^{3+}$ ion in 0.0093 M $HClO_4$ at four single-crystal gold electrodes: Au(210); Au(110) shifted downward by -10 μA; Au(100) shifted downward by -18 μA; and Au(111) shifted downward by -26 μA for better visualization. The electrode potential was scanned continuously in the range from -0.35 to $+1.25$ V vs $CE_{0.05}$ at a rate 20 mV s^{-1}, $t = 25$ °C. Arrows indicate the position of the potential of zero charge.

The irreversible one-electron reduction kinetics of $[Co(NH_3)_6]^{3+}$ ion at three different concentrations of perchloric acid was studied by cyclic voltammetry at a scan rate of 20 mV s^{-1}. Double-layer capacitance data were obtained by the same technique at $\upsilon = 50$, 100, and 200 mV s^{-1} from CVs in the range -0.5 and $+0.5$ V against the $CE_{0.05}$. Continuous cycling between -0.35 and $+1.25$ V against the $CE_{0.05}$ was adopted in both the presence and absence of the Co(III) species at $\upsilon = 20$ mV s^{-1}. The cycling procedure led to greater reproducibility of the kinetic data and ensured that the observations were predominantly conducted on unreconstructed (1×1) gold surfaces.

The reversibility of $[Ru(NH_3)_6](ClO_4)_3$ redox kinetics (CVs of 5×10^{-4} M solutions, $D_o = 5.52 \times 10^{-6}$ cm^2 s^{-1} at 25 °C, taken from Iwasita et al.[13]) was used to find the effective surface area of the electrodes. This reaction also provided some idea about any liquid junction potential shifts due to the different concentrations of perchloric acid used. The effective surface areas of the gold electrodes were 0.081 ± 0.001 cm^2 Au(111), 0.099 ± 0.002 cm^2 Au(100), 0.097 ± 0.003 cm^2 Au(110), and 0.103 ± 0.004 cm^2 Au(210), respectively. The liquid junction contributions were calculated by using the Henderson equation.[14] Data in Figures 1−3 were not corrected for liquid junction and are shown as measured. In all subsequent figures the potential scale is corrected for the liquid junction potential.

Results

Figure 1 shows cyclic voltammograms obtained for a solution of 5×10^{-4} M $[Co(NH_3)_6](ClO_4)_3$ in 0.0093 M $HClO_4$ at four single-crystals of gold Au(111), Au(100), Au(110), and Au(210) under the same experimental conditions. The curves are shifted vertically for better visualization. The arrows indicate the positions of the potential of zero charge (E_z), measured in 0.0093

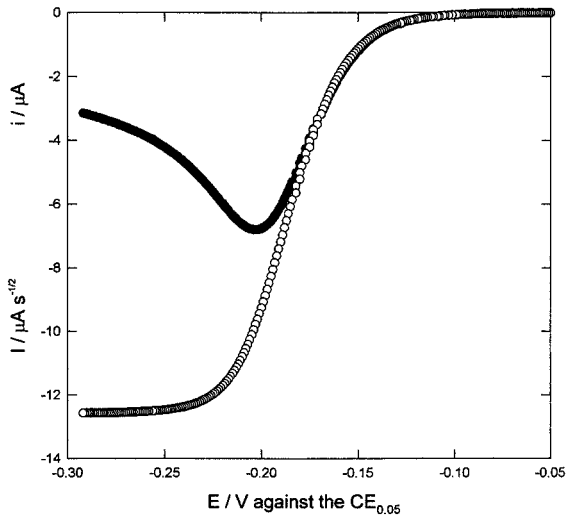

Figure 2. Part of the cyclic voltammogram corresponding to the reduction of 5×10^{-4} M $[Co(NH_3)_6]^{3+}$ ion in 0.093 M $HClO_4$ at Au(210) electrode (full circles) and the semmiintegral of this reduction current (empty circles). The experimental conditions were the same as in Figure 1.

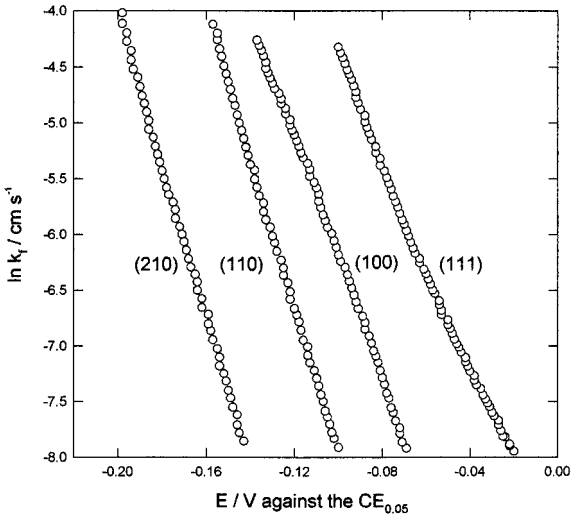

Figure 3. Logarithmic plot of the reduction rate constants for 5×10^{-4} M $[Co(NH_3)_6]^{3+}$ ion in 0.0093 M $HClO_4$ at four single-crystal gold substrates as a function of the experimental electrode potential.

M $HClO_4$ electrolyte under the same conditions. These E_z values, given in Table 2, are in good agreement with literature data.[5,15−20] Very good reproducibility of the reduction kinetics can be achieved via continuous cycling of the applied potential into the oxide formation region. It brings an additional benefit of permitting the assessment and maintenance of the desired quality of the electrode surface in the presence of the electroactive species.

As shown in Figure 1 the reduction kinetics of $[Co(NH_3)_6]^{3+}$ ion with 0.0093 M $HClO_4$ as supporting electrolyte depends on the crystallographic orientation of the gold. The peak potentials (E_p) are shifted toward more positive values as the substrate is changed from Au(210) to Au(110), Au(100), and Au(111). The decrease of the reduction peak currents (i_p) also indicates changes in the experimental transfer coefficients (α_{ex}) which correlate with the differences in the potential of zero charge. Reduction of 5×10^{-4} M $[Co(NH_3)_6]^{3+}$ was also measured in 0.0372 and 0.093 M $HClO_4$ electrolyte under the same conditions as in Figure 1.

From the cyclic voltammetric data the rate constants were extracted assuming a totally irreversible reduction process using the expression

$$\ln k_f = -\ln\left[\frac{I_{lim} - I(t)}{i(t)}\right] + \ln D_o^{1/2} \qquad (1)$$

where $I(t)$ is the semiintegral of $i(t)$ and D_o is the diffusion coefficient of the $[Co(NH_3)_6]^{3+}$ ion. Semiintegration was carried out as described in the literature.[21−23] The diffusion coefficients were based on literature data.[24,25] After corrections for the ionic strength used in our experiments,[26] values of D_o equal to 8.57×10^{-6}, 8.16×10^{-6}, and 7.76×10^{-6} cm^2 s^{-1} for $[Co(NH_3)_6]^{3+}$ ion were obtained in 0.0093, 0.0372, and 0.093 M $HClO_4$ solutions, respectively. Figure 2 shows a typical cyclic voltammogram and the corresponding semiintegral of the reduction current. The quality of the experimental data is exceptionally good allowing an analysis that does not require any prior knowledge of the dependence of the rate constant on electrode potential.

Figure 3 shows the logarithm of the forward rate constants as a function of applied potential for $[Co(NH_3)_6]^{3+}$ reduction obtained from the data in Figure 1. The rate constants at any chosen potential depend on the crystallographic orientation of the gold electrode. For example, at a constant potential of −0.1 V against the $CE_{0.05}$ reference electrode, the values of k_f are 1.3×10^{-2}, 2.1×10^{-3}, 3.7×10^{-4}, and 9.5×10^{-6} cm s^{-1} for Au(111), Au(100), Au(110), and Au(210) electrodes. This means that the electron-transfer to $[Co(NH_3)_6]^{3+}$ ion is fastest on Au(111) and slowest on Au(210) electrode at fixed electrode potential.

The experimental transfer coefficients (α_{ex}) can be obtained from the data in Figure 3, since

$$\alpha_{ex} = -\frac{1}{f}\frac{d \ln k_f}{dE} \qquad (2)$$

where $f = F/RT$ (38.92 V^{-1} at $t = 25$ °C). The logarithms of the rate constants do not deviate from linearity in the case of Au(210) and Au(110) electrodes, slight deviations are observed around the potential of zero charge for the Au(100) and Au(111) electrodes. From the linear parts of the logarithmic plots in Figure 3 values of α_{ex} equal to 1.74 ± 0.01, 1.68 ± 0.01, 1.38 ± 0.02, and 1.32 ± 0.05 were obtained for the Au(210), Au(110), Au(100), and Au(111) electrodes, respectively, indicating that the α_{ex} values increase from Au(111) to Au(210). The same data in Figure 3 can be replotted on the rational potential scale, $\phi^m = E - E_z$, in which case the rate constants at any given rational potential, say $\phi^m = 0$, increase from Au(111) to Au(210), that is, in the opposite order.

Figure 4 compares the logarithmic plots of the double-layer uncorrected rate constants on the rational potential scale for the reduction of 5×10^{-4} M $[Co(NH_3)_6]^{3+}$ ion at three different concentrations of supporting electrolyte at the Au(210) electrode. The rate constants for $[Co(NH_3)_6]^{3+}$ reduction decrease with decreasing concentration of the supporting electrolyte. The α_{ex} values are much larger than 1.0 in each case and increase with decreasing concentration of the electrolyte. The values of both α_{ex} and the reduction rate constants, obtained at −0.16 V against the $CE_{0.05}$ electrode, are summarized in Table 1. The peak potentials (E_p) in the CVs shift toward more negative values with decreasing concentration of the supporting electrolyte, consistent with the faster kinetics at higher concentrations. Qualitatively similar trends in the dependence of k_f values on the concentration of supporting electrolyte are observed for the

TABLE 1: Comparison of the Reduction Kinetics of 5×10^{-4} M $[Co(NH_3)_6]^{3+}$ Cation at Three Different Concentrations of Supporting Electrolyte on Au(210), Au(110), Au(100), and Au(111) Single-Crystal Electrodes

	α_{ex}				k_f/cm s^{-1}			
$[HClO_4]$	(210)	(110)	(100)	(111)	(210)[a]	(110)[a]	(100)[a]	(111)[a]
0.0093	1.74 ± 0.01	1.68 ± 0.01	1.38 ± 0.02	1.32 ± 0.05	2.7×10^{-3}	2.0×10^{-4}	1.5×10^{-4}	7.9×10^{-4}
0.0372	1.62 ± 0.01	1.61 ± 0.01	1.25 ± 0.02	1.29 ± 0.05	3.3×10^{-3}	2.8×10^{-4}	1.2×10^{-4}	6.3×10^{-4}
0.093	1.51 ± 0.01	1.41 ± 0.01	1.20 ± 0.02	1.24 ± 0.05	4.5×10^{-3}	3.6×10^{-4}	1.2×10^{-4}	5.5×10^{-4}

[a] Experimental rate constants obtained at constant, liquid junction corrected, electrode potential for all three electrolyte concentrations. Values of the potential were chosen for each electrode in the range where no extrapolation of k_f values is necessary, that is, at -0.16 V against the $CE_{0.05}$ for Au(210), at -0.08 V for Au(110), at -0.04 V for Au(100), and at -0.03 V for Au(111) electrode.

TABLE 2: Summary of Experimental Data from Corrected Tafel Plots for the Reduction of $[Co(NH_3)_6]^{3+}$ Cation at Au $\langle hkl \rangle$ Electrodes[a]

electrode	E_z/V	k^o_f/cm s^{-1}	α_a
Au(111)	$+0.07_4$	$(8.1 \pm 0.1) \times 10^{-7}$	1.05 ± 0.05
Au(110)	-0.17	0.022 ± 0.0003	1.05 ± 0.02
Au(210)	-0.24_6	0.43 ± 0.01	1.10 ± 0.01

[a] The kinetic parameters were obtained from cTps assuming $z = 2$. k^o_f is the value of the rate constant at the potential of zero charge ($\phi^m - \phi^d = 0$). The values of α_a and k^o_f at the Au(111) electrode were obtained from the linear parts of corrected Tafel plots.

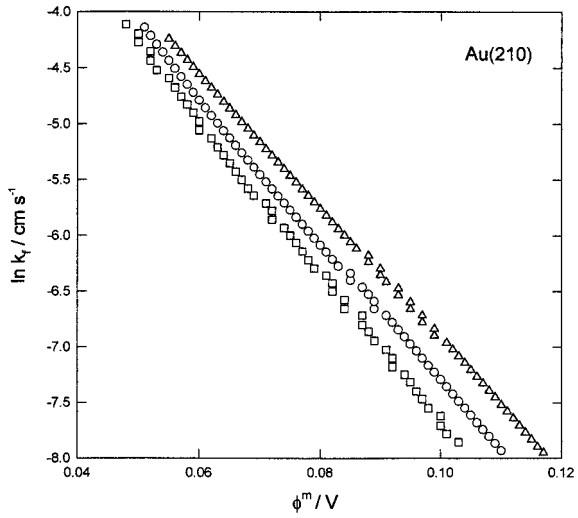

Figure 4. Plot of the logarithm of the rate constants for the reduction of 5×10^{-4} M $[Co(NH_3)_6]^{3+}$ at the Au(210) electrode at three different concentrations of perchloric acid: 0.093 M (△), 0.0372 M (○), and 0.0093 M (□) as a function of the rational potential $\phi^m = E - E_z$.

Au(110) and Au(100) electrodes, but the opposite trend is found for the Au(111) electrode (see Table 1). This behavior can be linked to the presence of negative charge densities on the Au(111) electrode during the reduction process as opposed to the positive values found at Au(210), Au(110), and Au(100) electrodes (see also Figure 1). The α_{ex} values for all four electrodes are also summarized in Table 1. They were obtained from the slopes of logarithmic plots such as those in Figure 4. Only the linear parts of logarithmic plots were used to evaluate α_{ex} in Table 1. However, it should be stressed that no assumption was made regarding the form of the electron-transfer kinetics law in correcting the data for the double-layer effects.

Kinetic data were corrected for the double-layer effects using the classical Frumkin approach. Capacitance data were obtained from the charging currents in the double-layer region. Figure 5 shows a set of capacitance curves for the Au(210) electrode assuming that the minimum on the curves corresponds to zero charge density on the electrode. The absence of specific adsorption of the perchlorate ions was assumed in the potential range of interest.[27] The experimental charge densities (σ_m) were

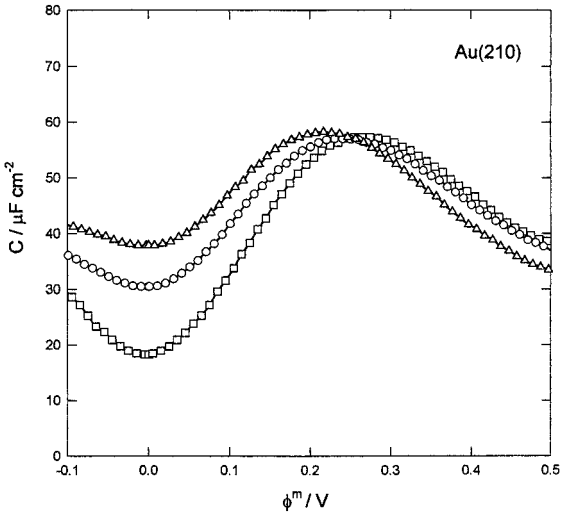

Figure 5. Capacitance curves obtained from the cyclic voltammograms at the Au(210) substrate at a scan rate of 100 mV s^{-1}, $t = 25$ °C, and for the three different concentrations of perchloric acid: 0.093 M (△), 0.0372 M (○), and 0.0093 M (□).

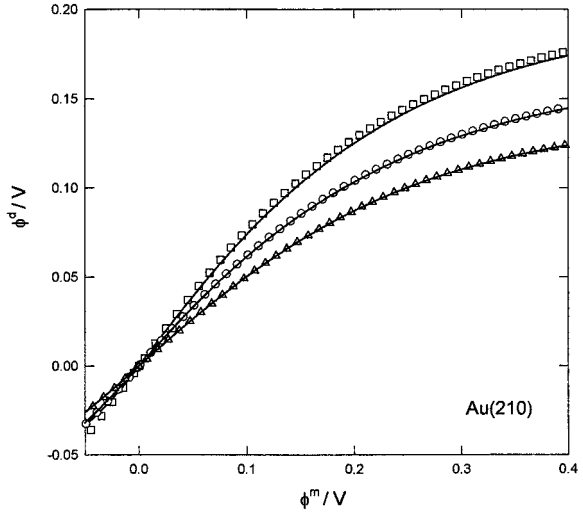

Figure 6. Diffuse-layer potential ϕ^d as a function of the rational potential ϕ^m for three concentrations of perchloric acid: 0.093 M (△), 0.0372 M (○), and 0.0093 M (□). The data represented by symbols are based on Figure 5 and the lines correspond to ϕ^d values corrected for the presence of the reactant and product of charge $z = 2$ in the diffuse layer.

calculated from these curves by integration and the potential on the outer Helmholtz plane (ϕ^d) was estimated by using the Gouy−Chapman theory. Figure 6 shows the resulting ϕ^d values for Au(210) on the rational potential scale. Figure 7 shows the dependence of the charge density at the electrode as a function of the potential drop across the inner layer. The values of σ_m fall approximately on one curve for all three concentrations of the supporting electrolyte. This is a strong indication that ionic

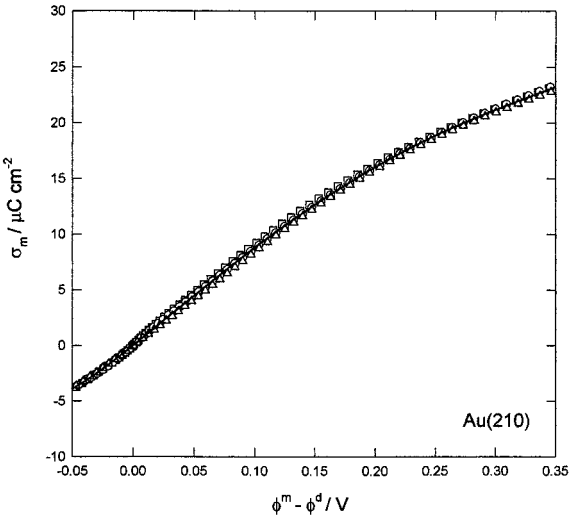

Figure 7. Charge density on the metal as a function of the potential drop across the inner layer for three concentrations of perchloric acid: 0.093 M (△), 0.0372 M (○), and 0.0093 M (□).

specific adsorption is absent at the Au(210) electrode over the range of charge densities studied.

Since the formation of ion pairs between the $[Co(NH_3)_6]^{3+}$ cation and the perchlorate anion cannot be excluded,[28] both $z = 3+$ and $z = 2+$ were assumed to be the charge on the reactant in analysis of the experimental data.

The reduction of $[Co(NH_3)_6]^{3+}$ ion at the Au(210) electrode proceeds at potentials sufficiently far from E_z, so that the presence of the reactant and the product in the double layer was included in the calculation of ϕ^d (see full lines in Figure 7). The values of ϕ^d in Figure 7 reflect the case where the predominant form of the reactant in the double-layer has a charge $z = 2+$. ϕ^d values in the presence of reactants and products were obtained by solving the equation [29]

$$\sigma_m^2/\theta^2 = c_s\Phi + c_d\Phi^2 + (c_s + 2c_d)/\Phi - 2c_s - 3c_d \quad (3)$$

numerically. σ_m is the charge density on the metal, $\Phi = \exp(-f\phi^d)$, c_s is the concentration of the supporting electrolyte, c_d is the concentration of the reactant, and $\theta^2 = 2RT\epsilon_s\epsilon_o$, where ϵ_s is the relative permittivity of the solvent and ϵ_o is the permittivity of free space. In case of the Au(210) electrode the difference between ϕ^d values corrected for the presence of reactants and products of charge 2+ and ϕ^d values obtained for pure supporting electrolyte is not very large, a slightly bigger difference being obtained for the Au(111) electrode, which is negatively charged during the reduction process.

In a crude way, Figure 7 illustrates that the decrease of the $[Co(NH_3)_6]^{3+}$ reduction rate upon decrease in the concentration of supporting electrolyte at the Au(210) electrode (see Table 1) can be associated with an increase in the diffuse layer potential at the OHP. ϕ^d has a positive value in the potential range of interest and the reduction of an approaching reductant, carrying a high positive charge, is slowed as a response to the increasingly positive potential at the outer Helmholtz plane. This type of double-layer effect most likely falls into the category of type II,[2] since a positively charged reactant is being reduced in the environment of the negatively charged perchlorate counterions. Under these circumstances the resulting ion−ion interactions should be attractive. The reduction of $[Co(NH_3)_6]^{3+}$ ion at the Au(110) and Au(100) electrodes also falls in the same category. On the other hand, $[Co(NH_3)_6]^{3+}$ ion is reduced at the Au(111) electrode at negative charge densities and the reacting cation is surrounded in the vicinity of the OHP by cations. This corresponds to a type I double-layer effect.[2]

Finally, the corrected Tafel plots (cTps) for Au(210) electrode are shown in Figure 8. These plots represent the corrections for the double-layer effects assuming that the reactants are point charges of $z = 3+$ (see Figure 8a) and $z = 2+$ (see Figure 8b) that are being reduced at the OHP. It is obvious from Figure 8 that the double-layer effects are quantitatively accounted for only if one assumes that the reacting species at the Au(210) electrode have predominantly a charge $z = 2+$. The corrected reduction rates in Figure 8b show a linear dependence on the potential drop across the inner layer, which can be expressed as

$$\ln k_f + zf\phi^d = \ln k^o_f - \alpha_a f(\phi^m - \phi^d) \quad (4)$$

where $z = 2$, α_a is the apparent transfer coefficient, and k^o_f is the reaction rate when both the ϕ^m and ϕ^d values are equal to zero. Based on this equation, the value of α_a is found to be 1.1 ± 0.01. The same method of data analysis was used for Au(110), Au(100), and Au(111) electrodes. The α_a values as well as k^o_f values for three of these electrodes, namely, Au(210), Au(110), and Au(111), are summarized in Table 2.

Significant difficulties were encountered with the analysis of the Au(100) data and this electrode was excluded for now from the quantitative treatment of the double-layer effects. This decision stems from the fact that sufficiently accurate capacitance data could not be obtained. As known from the literature,[19,20,30−32] surface reconstruction can be induced electrochemically at both Au(100) and Au(111) surfaces. However, the differences between the E_z values of reconstructed and unreconstructed surfaces are more than 100 mV larger for the Au(100) than for the Au(111) electrode. An additional complication arises due to the redox properties of the $[Co(NH_3)_6]^{3+}$ ion at the Au(100) electrode. The reduction of $[Co(NH_3)_6]^{3+}$ ion takes place around the potential of zero charge, where large errors in the estimate of the electrode charge density by integration are inevitable.

The double-layer corrected rate constants for the reduction of $[Co(NH_3)_6]^{3+}$ ion at the Au(210), Au(110), and Au(111) electrodes are shown in Figure 9 on the $E - \phi^d$ scale. The corrected Tafel plots for Au(111) are not linear, irrespective of the assumed value of the charge on the reactant. The double-layer effects at the Au(111) electrode are expected to be complex, because the electrode is negatively charged and both the species with $z = 2+$ as well as $z = 3+$ can be simultaneously reduced. Furthermore, the distribution of these ions at the electrode/electrolyte interface is expected to change with electrode potential. In addition, the presence of some reconstructed Au(111)(hex) surface cannot be completely excluded. However, we have tried to eliminate the presence of the reconstructed surface by subjecting the electrode to potentials positive enough to ensure that the reconstruction is lifted (see Figure 1). In Figure 9 the corrected kinetic data were obtained assuming that z equals 2+ in the entire potential range. Since any correction of the experimental data entails large errors in the vicinity of the E_z, the corrected rate constants for the $\phi^m - \phi^d$ values further from $\phi^m = E - E_z = 0$ should give more reliable numerical results. Based on this assumption, α_a was found to be 1.05 ± 0.05 for Au(111) in the region where the corrected Tafel plots overlap and approach linearity (see Figure 9). A straight line through these points gave a value of $k^o_f = (8.1 \pm 0.1) \times 10^{-7}$ cm s^{-1} at $\phi^m - \phi^d = 0$. Table 2 gives a summary of α_a and k^o_f values based on cTps for the Au(210), Au(110), and Au(111) electrodes.

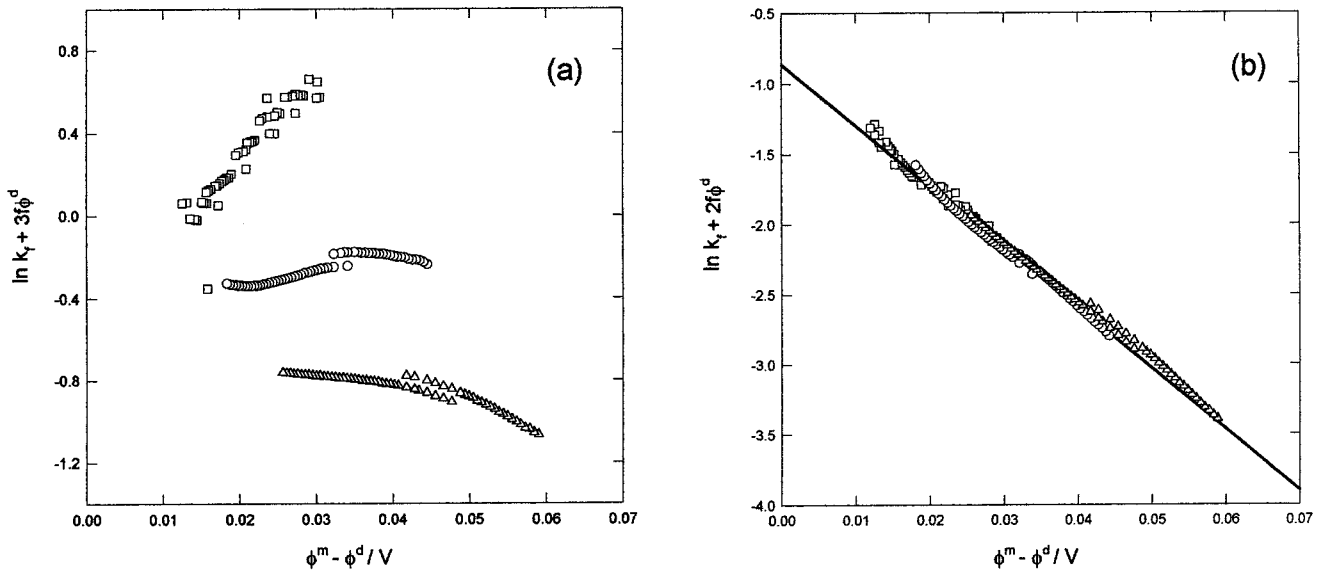

Figure 8. Corrected Tafel plots for the reduction of 5×10^{-4} M $[Co(NH_3)_6]^{3+}$ ion at the Au(210) electrode at three concentrations of perchloric acid: 0.093 M (△), 0.0372 M (○), and 0.0093 M (□) as a function of the potential drop across the inner layer. The charge on the reactant is assumed to be +3 (a) or +2 (b).

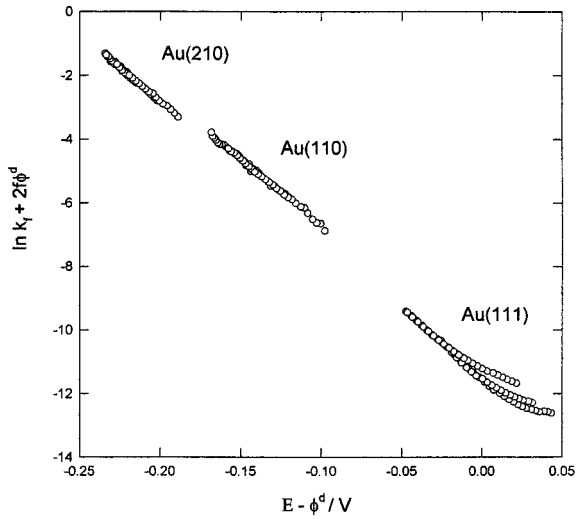

Figure 9. Corrected Tafel plots for the reduction of 5×10^{-4} M $[Co(NH_3)_6]^{3+}$ ion at Au(210), Au(110), and Au(111) electrodes at three concentrations of the supporting electrolyte plotted on the $E - \phi^d$ scale.

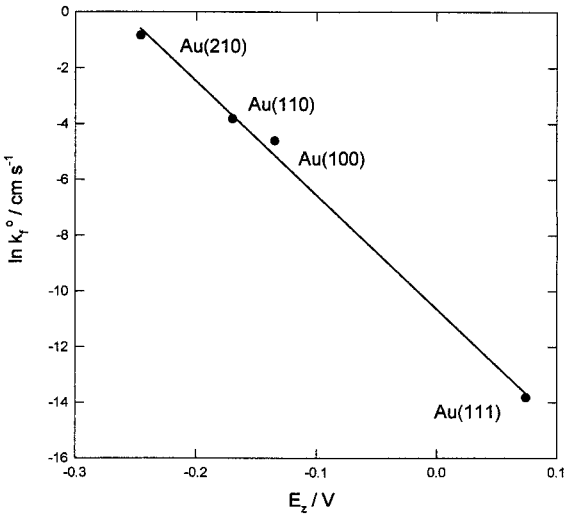

Figure 10. Semilogarithmic plot of the rate constants k^o_f (at $\phi^m = \phi^d = 0$) for the reduction of $[Co(NH_3)_6]^{3+}$ ion at four single-crystal gold electrodes as a function of the potential of zero charge of the electrode.

The data presented in Figure 9 suggest that the properly corrected reduction kinetics of $[Co(NH_3)_6]^{3+}$ ion depend on the crystallographic orientation of the gold substrate only through the differences in their potentials of zero charge. All three cTps are expected to have the same value of the rate constant at the formal/standard potential of the $[Co(NH_3)_6]^{3+/2+}$ reaction, which is confirmed in Figure 9 within the uncertainty limits of the kinetic parameters obtained. Additionally, values of the corrected rate constants at any chosen potential $E - \phi^d$ are the same for all three electrodes within the uncertainty limit of the corrected kinetic data. For example, a value of $(1.0 \pm 0.2) \times 10^{-3}$ was found at $E - \phi^d = -0.1$ V. This behavior is that expected for an outer-sphere adiabatic electron-transfer process. Unfortunately, due to the chemical irreversibility of the $Co(NH_3)_6^{3+/2+}$ process, the formal potential for this couple could not be determined. Thus, it was not possible to assess the present results on a potential scale related to the overpotential.

Figure 10 shows a semilogarithmic plot of the rate constant k^o_f at ϕ^m equal to zero (ϕ^d equal to zero as well) as a function of the potential of zero charge for all four electrodes. The rate constant k^o_f at Au(100) electrode obtained at the experimental value of E_z is also included. The dependence in Figure 10 is linear with a slope of -42.8 V^{-1} giving a value of α_a equal to 1.1.

Discussion

In this study, extremely large values of α_a have been obtained for the double-layer corrected reduction of the $[Co(NH_3)_6]^{3+}$ ion at all three gold substrates. This result is qualitatively the same as earlier observations at mercury[3,12,29] and gold.[3,33] The difference between the apparent transfer coefficient and an assumed true transfer coefficient of 0.5 was explained for the mercury electrode[29,34] by locating the reaction site in the inner layer. The relationship[2,35] between these quantities is

$$\alpha_a = \alpha - \lambda(\alpha - z) \qquad (5)$$

where α is the true transfer coefficient and λ a fraction giving the portion of the potential drop across the inner layer, $\phi^m - \phi^d$, which is added to ϕ^d to give ϕ^r, the potential at the reaction

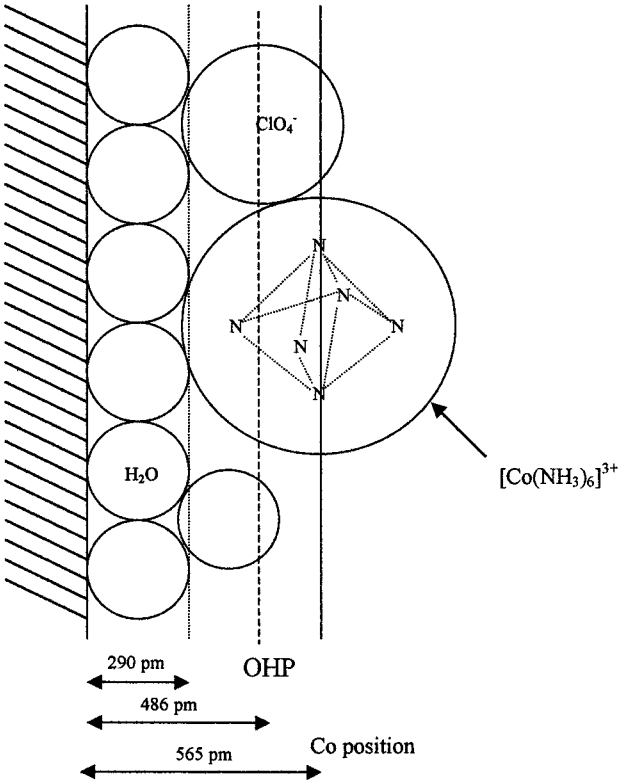

Figure 11. Simplified representation of the electrode/electrolyte interface at positive charge densities in the presence of $[Co(NH_3)_6]^{3+}$ reactant in the double-layer.

site. For the present results with α_a equal to 1.1, the corresponding value of λ is 0.4 when α is assumed to be 0.5. This would mean that the charge center of the reactant is well inside of the OHP at a position where it experiences 40% of the inner layer potential drop. However, this situation is not possible on purely geometric grounds (see Figure 11). Assuming that the electrode is covered by a monolayer of water molecules with an approximate diameter of 290 pm[36,37] and that the position of the OHP is determined by a perchlorate ion with a diameter of 452 pm, the thickness of the inner layer is approximately 486 pm. Assuming that the diameter of the $[Co(NH_3)_6]^{3+}$ complex is 598 pm[38,39] its cobalt atom should be located outside of the OHP at a distance of 565 pm from the geometrical interface. The chief approximation involved in developing this model of the area surrounding the reaction site is the assumption that all molecules and ions can be represented as hard spheres. This approach should not result in qualitative errors in the description of the double-layer effects.

For an alternative explanation of the high apparent transfer coefficients we adopted an approach outlined recently by Tsirlina et al.[40−42] They calculated the distribution of charge within a reactant using quantum mechanics and used it to obtain an improved estimate of the electrostatic energy of the reactant at the reaction site. To a first approximation, the reactant and product can be treated as a set of point charges at the different distances from the electrode surface. The work done (in dimensionless units) to bring the reactant to the reaction site is then

$$w_r = \sum_i z_i f\phi^i \tag{6}$$

where ϕ^i is the average potential at location i, z_i is the corresponding point charge, and the sum includes all point charges so that

$$z_r = \sum_i z_i \tag{7}$$

z_r being the charge on the reactant. The corresponding expressions for the product are

$$w_p = \sum_j z_j f\phi^j \tag{8}$$

where the charge on the product species is

$$z_p = \sum_j z_j \tag{9}$$

The expression for the forward rate constant can now be written as

$$\ln k_f = \ln k^o_f - w_r - \alpha(f\phi^m - w_r + w_p) \tag{10}$$

The experimental transfer coefficient is given by

$$\alpha_{ex} = -\frac{1}{f}\frac{d\ln k_f}{d\phi^m} = \alpha + \frac{1}{f}\frac{d[(1-\alpha)w_r + \alpha w_p]}{d\phi^m} \tag{11}$$

Assuming that α is equal to 0.5, the second term on the right-hand side gives a large positive contribution to the experimentally observed transfer coefficient α_{ex}. This contribution depends on the nature of the gold substrate and electrolyte concentration but is approximately independent of potential over the potential region studied. This suggests that a simple way of writing eq 9 is

$$\ln k_f = \ln k^o_f - w_a - \alpha f\phi^m \tag{12}$$

where w_a is the average work of transporting the reactant and product to the reaction site defined as

$$w_a = (1-\alpha)w_r + \alpha w_p \tag{13}$$

Thus, the expression for α_{ex} can also be simplified to

$$\alpha_{ex} = \alpha + \frac{1}{f}\frac{dw_a}{d\phi^m} \tag{14}$$

According to the classical Frumkin approach, the observed rate constant is corrected for the double-layer effect assuming that the reactant is a point charge and that the reaction site is at the OHP. The corresponding corrected Tafel plot (cTp) is

$$\ln k_f + z_r f\phi^d = \ln k^o_f + (z_r - \alpha)f\phi^d - w_a - \alpha f(\phi^m - \phi^d) \tag{15}$$

The slope of the corrected Tafel plot gives the apparent transfer coefficient α_a which is

$$\alpha_a = -\frac{1}{f}\frac{d(\ln k_f + z_r f\phi^d)}{d(\phi^m - \phi^d)} = \alpha - (z_r - \alpha)\frac{d\phi^d}{d(\phi^m - \phi^d)} + \frac{1}{f}\frac{dw_a}{d(\phi^m - \phi^d)} \tag{16}$$

The second term on the right-hand side of eq 15, which gives the classical double-layer effect, corresponds to a negative contribution to α_a. The third term, which is part of the true double-layer effect, corresponds to a much larger positive

contribution to α_a and can be obtained only through detailed knowledge of the distribution of charges within the reactant and product. Since the dependence of w_a on ϕ^m cannot be calculated at this time, only a rough estimate of α_a through the parameter λ is shown below.

It is assumed that the electronic charge 3+ is equally distributed among the six NH_3 groups of $[Co(NH_3)_6]^{3+}$, that is, +0.5 on each ammino group. This assumption is not unreasonable, since similar values were found by Iwata[43] using an X-ray analysis of $[Co(NH_3)_6]$ $[Co(CN)_6]$ crystals. The $[Co(NH_3)_6]^{3+}$ ion is assumed to be separated from the electrode surface by a layer of interfacial water molecules and the center of the ClO_4^- counterion defines the OHP at $x^d \approx 486$ pm. The ratio $\sum z_i f \phi^i / z f \phi^d$ was calculated for $[Co(NH_3)_6]^{3+}$ reduction at the Au(210) electrode in 0.093 M $HClO_4$ (at $\sigma_m = 3.3$ μC cm^{-2}) for three arrangements of the $[Co(NH_3)_6]^{3+}$ octahedron in the double-layer (apex, edge, and wall) and compared with the ratio $\phi^r/\phi^d \approx 1.35$ which is expected for λ equal to 0.4. An apex arrangement corresponding to one NH_3 group in the immediate vicinity of the water layer and four in the plane of the cobalt atom, about 80 pm away from the OHP, gave the closest agreement with the desired ϕ^r/ϕ^d value.

The reduction of $[Co(NH_3)_6]^{3+}$ ion is a very interesting system which gives exceptionally large double-layer effects at gold electrodes. For example, on mercury these effects are smaller in magnitude.[3,25] Contrary to the case with the mercury electrode, the double-layer effects cannot be explained with the simple assumption that the reactant is a point charge. The high values of α_a can be rationalized for this system assuming a distribution of charges within the $[Co(NH_3)_6]^{3+}$ ion. The present data are consistent with a picture of the double-layer in which the central cobalt atom is located just outside the OHP and forms an associate with the perchlorate ion during the transport process through the double-layer. Since ion pairing makes a quantitative analysis of the double-layer effects more complicated, the less positively charged $[Co(NH_3)_5F]^{2+}$ system is currently being investigated at the same gold electrodes. This ion can also serve as an interesting system with respect to the effects of charge distribution in the reactant, since the charge in the $[Co(NH_3)_5F]^{2+}$ ion is not symmetrically distributed.

Finally, the corrected Tafel plots indicate that the reduction of the $[Co(NH_3)_6]^{3+}$ ion depends on the crystallographic orientation of the gold substrate only through the differences in the potentials of zero charge. This behavior is consistent with the assumption that the reduction of $[Co(NH_3)_6]^{3+}$ ion is an adiabatic process.

Acknowledgment. We are indebted to Dr. G. A. Tsirlina for stimulating discussions of charge distribution effects in the electrode kinetics. This work was supported by a grant from the National Science Foundation (CHE-9729314).

References and Notes

(1) Fedorovich, N. V. *Reports in Science and Technology*, *Electrochemistry*; Viniti: Moscow, 1979; Vol. 14, p 5 (in Russian).
(2) Fawcett, W. R. *Electrocatalysis*; Lipkowski, J., Ross, P. N., Eds.; Wiley-VCH: New York, 1998; p 323.
(3) Hamelin, A.; Weaver, M. J. *J. Electroanal. Chem.* **1986**, *209*, 109.
(4) Hamelin, A.; Weaver, M. J. *J. Electroanal. Chem.* **1987**, *223*, 171.
(5) Brug, G. J.; Sluyters-Rehbach, M.; Sluyters, J. H.; Hamelin, A. *J. Electroanal. Chem.* **1984**, *181*, 245.
(6) Perez, J.; Gonzales, E. R.; Villullas, H. M. *J. Phys. Chem. B* **1998**, *102*, 10 931.
(7) Fedorovich, N. V.; Levi, M. D.; Kulakovskaya, S. I. *Elektrokhimiya* **1977**, *13*, 904.
(8) Samec, Z.; Bittner, A. M.; Doblhofer, K. *J. Electroanal. Chem.* **1997**, *432*, 205.
(9) Fawcett, W. R.; Fedurco, M.; Kováčová, Z. *J. Electrochem. Soc.* **1994**, *141*, L30.
(10) Fawcett, W. R. *Electrochim. Acta* **1997**, *42*, 833.
(11) Samec, Z. *J. Electrochem. Soc.* **1999**, *146*, 3349.
(12) Tadayyoni, M. A.; Weaver, M. J. *J. Electroanal. Chem.* **1985**, *187*, 283.
(13) Iwasita, T.; Schmickler, W.; Schultze, J. W. *Ber. Bunsen-Ges. Phys. Chem.* **1985**, *89*, 138.
(14) Dvořák, J.; Koryta, J. *Electrochemie*; Academia: Praha, 1983; p 138 (in Czech).
(15) Hamelin, A. *J. Electroanal. Chem.* **1996**, *407*, 1.
(16) Hamelin, A.; Martins, A. M. *J. Electroanal. Chem.* **1996**, *407*, 13.
(17) Lecour, J.; Bellier, J. P.; Koehler, C. *Electrochim. Acta* **1990**, *35*, 1383.
(18) Motheo, A. J.; Sadkowski, A.; Neves, R. S. *J. Electroanal. Chem.* **1997**, *430*, 253.
(19) Kolb, D. M.; Schneider, J. *Electrochim. Acta* **1986**, *31*, 929.
(20) Eberhardt, D.; Santos, E.; Schmickler, W. *J. Electroanal. Chem.* **1996**, *419*, 23.
(21) Imbeaux, J. C.; Savéant, J. M. *J. Electroanal. Chem.* **1973**, *44*, 169.
(22) Savéant, J. M.; Tessier, D. *J. Electroanal. Chem.* **1975**, *65*, 57.
(23) Oldham, K. B. *J. Electroanal. Chem.* **1986**, *208*, 1.
(24) Lide, D. R. *Handbook of Chemistry and Physics*; CRC Press: Boca Raton, FL, 1998; pp 5−93.
(25) Fawcett, W. R.; Markušová, K. *Can. J. Chem.* **1983**, *61*, 2821.
(26) Robinson, R. A.; Stokes, R. H. *Electrolyte Solutions*; Butterworth: London, 1959.
(27) Calvente, J. J.; Marinković, N. S.; Kováčová, Z.; Fawcett, W. R. *J. Electroanal. Chem.* **1997**, *421*, 49.
(28) Högfeldt, E. *IUPAC Stability Constants of Metal Ion Complexes*, *Part A*, *Inorganic Ligands*; Pergamon Press: New York, 1982; p 248.
(29) Fawcett, W. R.; Markušová, K. *J. Electroanal. Chem.* **1989**, *270*, 119.
(30) (a) Schneider, J.; Kolb, D. M. *Surf. Sci.* **1988**, *193*, 579. (b) Kolb, D. M.; Schneider, J. *Surf. Science* **1985**, *162*, 764.
(31) Ross, P. N.; D'Agostino, A. T. *Electrochim. Acta* **1992**, *37*, 615.
(32) Ocko, B. M.; Wang, J.; Davenport, A. J.; Isaacs, H. S. *Phys. Rev. Lett.* **1990**, *65*, 1466.
(33) Barr, S. W.; Guyer, K. L.; Weaver, M. J. *J. Electroanal. Chem.* **1980**, *111*, 41.
(34) Satterberg, T. L.; Weaver, M. *J. Phys. Chem.* **1978**, *82*, 1784.
(35) Fawcett, W. R. *Can. J. Chem.* **1981**, *59*, 1844.
(36) Schmickler, W.; Henderson, D.; Melroy, O. R. *Chem. Phys. Lett.* **1993**, *216*, 424.
(37) Wang, J.; Ocko, B. M.; Davenport, A. J.; Isaacs, H. S. *Phys. Rev. B* **1992**, *46*, 10321.
(38) Newton, M. D. *J. Phys. Chem.* **1988**, *92*, 3049.
(39) Kalman, B. L.; Richardson, J. W. *J. Chem. Phys.* **1971**, *55*, 4443.
(40) Nazmutdinov, R. R.; Tsirlina, G. A.; Kharkats, Y. I.; Petrii, O. A.; Probst, M. *J. Phys. Chem. B* **1998**, *102*, 677.
(41) Tsirlina, G. A.; Kharkats, Y. I.; Nazmutdinov, R. R.; Petrii, O. A. *Elektrokhimiya* **1999**, *35*, 23.
(42) Khrushcheva, M. L.; Tsirlina, G. A.; Petrii, O. A. *Elektrokhimiya* **1998**, *34*, 355.
(43) Iwata, M. *Acta Crystallogr.* **1977**, *B33*, 59.